PROTRACTED GLOBAL CATASTROPHES FROM OBLIQUE IMPACTS; P.H. Schultz, Dept. Geological Sciences, Brown University, Providence, RI 02912 and D.E. Gault, Murphys Center of Planetology, P.O. Box 833, Murphys, CA 95247.

The hypothesis that impacts caused major climate and biologic catastrophes at the end of the Cretaceous faces numerous paradoxes including: evidence for protracted extinctions (1), non-uniform but widespread dispersal of the meteoritic signature, conflicting evidence for oceanic (2) and continental (3) impact sites, indications of intense fires (4), massive nitrate production (5), and the absence of a putative crater of sufficient size. Not every known major impact can be associated with a biologic catastrophe as extreme as at the close of the Cretaceous. Either a rare set of geologic/environmental conditions is needed to enhance the effects of a particular impact, or a rare but probable impact condition must be invoked to increase the climate/biologic response. The latter alternative is addressed here by exploring further the suggestion (6, 7) that an oblique impact could significantly amplify normally cited vertical impact. Cited collision rates implicitly assume a 45° impact angle. If a 10–km diameter impactor represents a 40 my event, then a 15° and 10° strike represent a 300 my and 670 my event, respectively. The fate of the projectile (physical state, fragmentation, dispersal) and coupling with the atmosphere are key issues that are addressed here.

Approach: Laboratory experiments permit exploring the partitioning of energy and projectile fate as a function of impact angle. Although such laboratory experiments are at small scale, they nevertheless establish the first–order relative effects of impact angle and provide an important reference for testing computational experiments. Two series of experiments were performed at the NASA–Ames Vetical Gun Range for a given impact size (0.635 cm) and type (aluminum): the first varied impact velocity (2–6.3 km/s) with a constant impact angle (15°); the second varied impact angle (2.5–30°) with constant impact velocity (5.5 km/s). Aluminum witness plates placed downrange registered the degree and distribution of projectile fragmentation. Scaling laws for impacts into aluminum over the same range of velocities (and including projectile size effects, 8) permitted converting apparent pit diameter (referenced to the pre–impact surface) into fragment mass and mean fragment velocity by an iterative solution. First, individual fragment mass was derived from pit diameter with the assumption that the ricochet velocity was equal to the initial impact velocity. The assumed impact velocity was then reduced iteratively until the total calculated fragment mass was equal to the original impactor mass. This approach presumes that all of the high–velocity ricochet debris is comprised of projectile rather than target fragments. Previous studies indicated that at low impact angles (<30°), projectile fragments dominate the downrange debris (9, 10); hence, this approach establishes a lower limit to the ricochet energy fraction (KE_p/KE_i). The derived ricochet energy added to the energy expended in excavating the crater in sand (ejecta plus compaction) as a function of impact angle demonstrated that total energy was conserved for the given impact conditions.

Fragmentation of a given projectile (type, size) was first examined as a function of specific energy ($Q = KE_i/m_p$ = projectile kinetic energy divided by projectile mass), thereby paralleling analyses of bulk fragmentation of large bodies by small impactors (11). The percentage of fragments larger than a given mass fraction (m_i/m_p) as a function of specific energy provides a measure of the degree of fragmentation. The onset of fragmentation should be reflected by either the largest fragment mass (m_L) or the mass fraction fragmented more than once ($1-m_L/m_p$). Derived cratering efficiencies into solid targets (9) suggest that the peak stress during impact varies as $\sin^2\theta$ where θ is the impact angle from the horizontal. Hence, the normal stress experienced by the projectile can be given by $\sin^{2n}\theta$ where n is derived either empirically or from physical considerations.

Results: Gault and Wedekind (9) previously demonstrated that projectile fragmentation depends on velocity and angle for a given projectile and target. The present analysis reveals two regimes of failure resembling disruption of larger suspended targets (12, 13): limited and complete. Limited disruption of the projectile is characterized by a single, large fragment (>0.3 m_p), whereas complete disruption is characterized by the largest fragment mass less than about 0.1 m_p. The simple expression $Q\sin^2\theta = 1/2\, v^2\sin^2\theta$ (i.e., n = 1) was found to accommodate the mass–frequency distribution of small fragments ($m_i/m_p < 0.01$ m) for both limited and complete disruption. The same function accommodated data for the largest single fragment mass provided that complete projectile disruption occurred, i.e., $\theta \succeq 15°$ and $v \succeq 4$ km/s. Limited disruption characterizing lower impact angles and velocities required a larger exponent, i.e., $Q\sin^6\theta$ (n = 3). This latter result can be shown to reflect the combined effects of three competing internal energy–loss processes in the projectile that cannot be neglected at very low impact angles. First, the maximum vertical compressive stress developed at impact reduces as $\sin^2\theta$ as derived either from balancing observed energy expended in crater excavation and kinetic energy in the ricochet fraction or from the impact–angle dependence on cratering efficiency in strength–limited targets. Second, a fraction of this transferred normal stress, however, will be lost due to shear heating along the projectile/target interface and will not be available for bulk projectile disruption. On the basis of an impact–angle dependence on vaporization of easily volatized targets (14), this factor also depends on $\sin^2\theta$. Third, multiple fragmentation and localized spallation of the projectile further reduces the specific energy available for complete catastrophic disruption. The frequency distribution of the smallest fragments produced during limited disruption indicates a $\sin^2\theta$ dependence as well. Hence, a $\sin^6\theta$ dependence can be derived for limited projectile disruption.

The distinction between limited and complete projectile disruption also could be viewed as a distinction between shock and mechanical failure at high and low stress levels (and strain rates), respectively. Moreover, conditions leading to projectile failure should resemble conditions leading to target failure. With these two perspectives, the two disruption regimes can be compared with data from Davis and Ryan (13). When complete shock–controlled disruption is assumed and a correction factor for impedance matching is included, conditions for complete disruption (high v and θ) lead to a close match between projectile disruption and target disruption, even with a factor of 20 contrast in object size and up to a factor of 60 in object strength. Conditions leading to limited disruption (low v and θ), however, are not accommodated. For limited disruption largely controlled by mechanical failure, data for low v and θ are now consistent for both data sets, whereas data for high v and θ are not. A single expression can be derived that incorporates both failure conditions.

Implications: At much broader scales, strain–rate and strength effects may be important and need to be introduced. Figure 1 has incorporated a nominal case derived in (15) using dimensional analysis and provides a first–order range of estimates for the largest fragment surviving a 20 km/s impact from an initial 10 km–diameter object as a function of impact angle. At the very least, Figure 1 indicates that the projectile signature could be carried downrange ballistically, rather than entrained in the ejecta. Because the ricochet angle is typically lower than the impact angle (9), this fraction would induce increased coupling with the atmosphere and could create a broad, long, and potentially intense fire–line largely decoupled from the impact site. At sufficiently low impact angles, a single, large impactor could spawn numerous smaller but still substantial ricochet fragments impacting a wide range of geologic settings. From the laboratory analyses, the ricochet velocities asymptotically approach about 0.5 v with increasing impact velocities at a given impact angle (15°). Consequently such fragments should produce a global deluge of hypervelocity debris re–entering the atmosphere and striking a variety of geologic settings. Because the consequences of low–angle impacts have not yet been fully explored, our interpretations could be considered in part speculative. Nevertheless, the mechanics and phenomena of low angle impacts are grossly different from the nominal high–angle impact scenarios and necessitate further serious study.

(1) Keller G. (1988) In *Global Catastrophes in Earth History*, pp 88-89. LPI Contrib. 673. (2) Hildebrand A.R. and Boynton W.V. (1988) In *Global Catastrophes in Earth History*, pp. 76-77. LPI Contrib. 673. (3) Sharpton V.L. *et al.* (1988) In *Global Catastrophes in Earth History*, pp. 172-173. LPI Contrib 673. (4) Wolbach W.S. *et al* (1985) *Science 230*, pp. 167-170. (5) Prinn R. and Fegley B. (1987) *Earth Planet. Sci. Letts 83*, pp. 1-15 (6) Schultz P.H. and Gault D.E. (1982) In *Geol. Soc. Am. Sp. Paper 190*, pp. 153-174. (7) Schultz P.H. and Gault D.E. (1988) In *Global Catastrophes in Earth History*, pp. 166-167. (8) Denardo P. *et al.* (1967) *NASA TN D-4067*. (9) Gault D.E. and Wedekind J.A. (1978) *Proc. Lunar Planet. Sci. Conf. 9th*, pp. 3843-3875. (10) Gault D.E. and Schultz P.H. (1986) *Meteoritics 21*, pp. 368-369. (11) Gault D.E. and Wedekind J.A. (1969) *J. Geophys. Res. 74*, pp. 6780-6794. (12) Fujiwara A. *et al.* (1977) *Icarus 31*, pp. 277-288. (13) Davis D.R. and Ryan E.V. (1988) On collisional disruption: Experimental results and scaling laws (preprint). (14) Schultz P.H. (1988) *Lunar and Planet. Sci. XIX*, pp. 1039-1040. Lunar and Planetary Institute, Houston. (15) Holsapple K.A. and Housen K.R. (1986) *Mem. S.A. It. 57*, pp. 65-85.

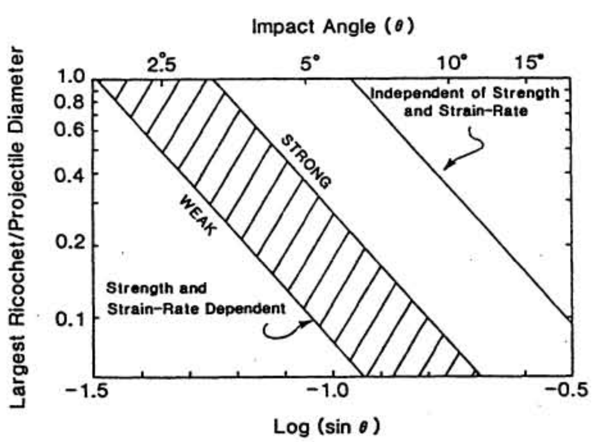

Figure 1. Size of the largest ricochet fragment surviving an oblique impact by a 10 km–diameter object at 20 km/s based on projectile and target fragmentation in the laboratory.